Sensors and Actuators B 266 (2018) 543–552

Contents lists available at ScienceDirect

Sensors and Actuators B: Chemical

journal homepage: www.elsevier.com/locate/snb

Biominerized gold-Hemin@MOF composites with peroxidase-like and gold catalysis activities: A high-throughput colorimetric immunoassay for alpha-fetoprotein in blood by ELISA and gold-catalytic silver staining

Liyan Zhang, Chuan Fan, Min Liu, Fengjuan Liu, Shanshan Bian, Shuyue Du, Shuyun Zhu, Hua Wang*

Institute of Medicine and Materials Applied Technologies, College of Chemistry and Chemical Engineering, Qufu Normal University, Qufu City, Shandong Province 273165, PR China

ARTICLE INFO

Article history:
Received 20 September 2017
Received in revised form 28 February 2018
Accepted 25 March 2018
Available online 27 March 2018

Keywords:
Gold biomineralization
MOF encapsulation
Hemin-Au@MOF composites
Peroxidase-like catalysis
Gold catalysis
Sandwiched AFP immunoassays

ABSTRACT

Catalytic hemin was first remolded with biomineralized gold to form Hemin-Au core and further encapsulated into the Tb metal organic framework (MOF) matrix. The so obtained Hemin-Au@MOF composites could possess high environmental stability and especially double catalysis activities of enhanced peroxidase-like and gold catalysis. Steady state kinetics studies indicate that Hemin-Au@MOF could present much higher intrinsic catalysis and substrate affinity (lower Michaelis constants) than native hemin and even natural peroxidase. Furthermore, the catalytic composites were employed for labeling antibodies towards the sandwiched immunoassays for alpha-fetoprotein (AFP) as a model biomarker of cancers. The results indicate that the Hemin-Au@MOF-based immunoassays could be conducted by two signal amplification ways of hemin-catalyzed chromogenic reaction and gold-catalyzed silver staining, enabling the detection of AFP in blood with the level down to 0.020 ng mL^{-1}. Importantly, the proposed fabrication protocol combining the gold biomineralization and MOF encapsulation routes may be extended for the fabrication of a variety of enzymes or enzymatic mimics with the improved environmental stability and multiple catalysis activities for the wide catalysis applications.

1. Introduction

The early diagnosis and therapy is of crucial importance for cancers. However, the cancer-sensitive biomarkers, i.e., alpha-fetoprotein (AFP), for making the diagnostic decision at the early stages may generally possess extremely low levels in human body fluids like blood, thus making the analysis a formidable issue entailing the sensitive and accurate detection methods [1]. Moreover, AFP is recognized to reflect the physiological state of a cancer serving as a very popular and sensitive "molecular signature". Too high AFP concentration in blood is a meaningful clinical symptom of malignant tumors like liver cancer. Up to date, many analytical methods have been developed for the detection of AFP, most known as the enzyme-linked immune-sorbent assay (ELISA), electrochemical luminescence [2], localized surface plasmon resonance [3], and colorimetric immunoassay [4]. Although these classic detection protocols can possess high analysis sensitivity, they are labor-intensive, time-consuming, and especially unsuitable for point-of-care analysis applications. Therefore, developing a rapid, sensitive, selective, and field-applicable detection candidate for the AFP analysis is of great interest for the clinical early diagnosis of various cancers.

There are two kinds of popular signal amplification ways of ELISA and gold catalyzed silver staining (GCSS) in the sandwiched immunoassays [5–8], which are also applied in the clinical laboratory for the evaluation of AFP in blood. It is recognized that the detection performances of these sandwiched analysis techniques can largely depend on the performances of catalytic labels of enzymes like horseradish peroxidase (HRP) or catalysts like gold nanoparticles (AuNPs) in ELISA and GCSS, respectively [9–11]. Particularly, enzymes like HRP were even modified with AuNPs to achieve the improved catalysis for the signal-amplified detections of DNAs or proteins [12,13]. The practical applications of enzymes, however, may be limited by their intrinsic disadvantages such as

* Corresponding author.
E-mail address: huawangqfnu@126.com (H. Wang).

https://doi.org/10.1016/j.snb.2018.03.153
0925-4005/

high cost, harsh storage, and easy deactivation in water. Considerable efforts have hence been devoted to the development of more robust enzymes or enzymatic alternatives for the design of various catalysis-based biosensors [14,15]. As the most interesting example, hemin, a cheap substitute of peroxidases commonly extracted from the active center of hemin-containing enzymes or catalytic proteins, has been applied for a variety of biocatalysis applications [16,17]. Unfortunately, hemin in aqueous media may still suffer from some inherent limitations such as poor aqueous solubility, ready destruction, and molecular aggregation (i.e., inactive dimers), showing the low catalysis activity [18]. As a result, some researchers have tried to improve the catalytic activity and aqueous stability of hemin by the organic modification [19,20] or by anchoring of some conductive materials [16,21,22]. For example, hemin was coupled onto graphene to yield the hemin-graphene hybrid showing improved catalysis activities [16]. Also, hemin was cross-linked with a protein scaffold to achieve the enhanced catalysis and aqueous stability [20].

Moreover, the GCSS-based analysis methods are generally established by using gold labels to catalyze the deposition of silver elements [23,24], leading to the signal amplification towards the sensitive biological detections [7,8,10,25,26]. Yet, the catalysis activities of noble metal nanomaterials like AuNPs can substantially depend on their particle sizes (i.e., smaller than 5.0 nm), known as the "size effects" [27–31]. Chen and his workers utilized AuNPs as the enzyme mimic for the sensitive immunoassays [30]. Park's group designed a hybrid structure of graphene-gold nanoparticles for the visible detection of norovirus-like particles [31]. Willner's group employed ultra-small AuNPs to modify enzymes serving as the "biocatalytic ink" to grow metallic nanowires by way of the GCSS [32]. More recently, our group encapsulated gold "nanowires" into alkalline phosphatase achieving greatly enhanced catalysis towards the GCSS-enabled signal amplification for ultrasensitive DNA analysis [8].

In recent years, metal-organic frameworks (MOFs) have concentrated increasing interests due to their unique porous structure, high surface areas, and tunable physicochemical properties [2,33,34]. In particular, functionalized MOFs have recently been applied as the functional carriers or coatings for the biosensing detections [35–38]. For instance, Ju's group employed DNA functionalized iron-porphyrinic MOF as the probe for an electrochemical detection of lead ions [36]. Liang and co-works discovered that enzymes like HRP could induce the formation of protective MOF coatings under physiological conditions, resulting in the greatly enhanced environmental robustness of enzymes [37]. Also, Yang et al. reported an electrochemical immunoassay for C-reaction protein by using Cu-MOF-labeled antibody [38].

Inspired by these pioneering works above, in the present work, the cheap catalytic hemin was extracted from the hemin-containing protein and then remolded with small AuNPs by the in-site gold biomineralization route. The so yielded Hemin-Au core was further encapsulated into the porous Tb-metal organic framework (Tb-MOF) matrix to produce the Hemin-Au@MOF composites (Scheme 1). It was discovered that the obtained Hemin-Au@MOF could possess greatly improved environmental stability and especially the double catalysis activities of peroxidase-like and gold catalysis. Herein, the so biomineralized gold would act as "nanowire" to promote the electron transferring of catalysis-active sites of Hemin-Au@MOF. The catalysis performances of Hemin-Au@MOF were investigated in comparison to those of native hemin and other peroxidases like HRP, including the kinetics studies. Furthermore, the prepared Hemin-Au@MOF composites were employed as the catalytic labels for modifying antibodies in the sandwiched immunoassays for AFP as a model biomarker of cancers by two signal amplification ways of hemin-catalyzed chromogenic reaction and gold-catalyzed silver staining. To the best of our knowledge, this is the first attempt of the successful synthesis of robust enzymatic composites with high environmental stability and substantially enhanced double catalysis activities for the sandwiched immunoassays through combining the gold biomineralization and MOF encapsulation routes.

2. Experimental section

2.1. Reagents and apparatus

Hemin, bovine serum albumin (BSA), 3,3′,5,5′-tetramethylbenzidine (TMB), TMB-H_2O_2 chromogenic substrate, chitosan (CS), and silver nitrate ($AgNO_3$) were purchased from Sigma-Aldrich (Beijing, China). Hydrogen tetrachloroaurate ($HAuCl_4$), citric acid, terephthalic acid disodium salt, $TbCl_3{\cdot}6H_2O$, ethanol, and phosphate buffer solution (PBS, pH 7.4) were obtained from Aladdin Reagent Co., Ltd. (Shanghai, China). Bovine serum albumin (BSA), alpha-fetoprotein (AFP), anti-AFP antibody were purchased from Sinopharm Cheminical Reagent Co. (China), while the Hemin-Au@MOF labeled anti-AFP antibody were prepared by cross-linking chemistry. The blood samples were kindly provided from the local hospital. Other chemicals were of analytical grade and used without further purification. Deionized water (>18 MΩ) was supplied from an Ultrapure water system (Pall, USA). Silver deposition substrates consisting of $AgNO_3$ (2.0 mM) and vitamin C (0.57 mM) were applied for the gold-catalytic silver staining.

Colorimetric measurements of the catalytic activities of the composites or enzymes were performed by a microplate reader (Infinite M200 PRO, Tecan, Austria) and 96-well plates (JET BIOFIL, Guangzhou, China). Transmission electron microscopy (TEM, FEI Tecnai G20, USA) imaging operated at 100 kV was employed to characterize the composites and nanomaterials. UV–vis absorption spectra with 96-well plates were collected for enzymatic activity analysis using UV-3600 spectrophotometer (Shimadzu, Japan) equipped with a thermostated holder. Thermostatic mixing was performed by DF101 collector-type temperature magnetic stirrer (Gongyi Corey Ltd.).

2.2. Synthesis of mimic enzymes of Hemin-Au@MOF composites

Hemin with biomineralized gold (Hemin-Au) cores were synthesized by the hemin-templated in-site gold biomineralization route according to the previous work [21]. Briefly, under vigorous stirring, $HAuCl_4$ (1.0 mL, 10 mM) was mixed with hemin solution (1.0 mL, 0.80 mg mL^{-1}), followed by the addition of an aliquot of NaOH (120 μL, 1.0 M). After the mixture was stirred for 8 h at 37 °C, the Hemin-Au was dialyzed in water for 8 h using the dialysis membranes with the pore size of 1.8 nm or molecular weight of 20 KD, of which the cut-off particle size or molecular weight was close to that of Hemin-Au. Finally, the so prepared Hemin-Au cores were stored at 4 °C for future usage. The Hemin-Au products were separately characterized by TEM imaging and UV–vis spectrophotometer. Furthermore, under vigorous stirring, the as-prepared Hemin-Au cores (0.50 mL, 0.080 mg mL^{-1}) were mixed with $TbCl_3{\cdot}6H_2O$ solution (1.0 mL, 10 mM), followed by the continuous stirring at room temperature for 15 min. An aliquot of BSA (10 mM) was added to the reaction solution to accelerate the formation reactions of MOF. Then, terephthalic acid disodium salt (1.0 mL, 10 mM) was introduced to be vigorously stirred for 2 h to form Hemin-Au@MOF composites. After being placed at 4 °C overnight, the yielded composites were centrifuged by the freeze drying (10000 r s^{-1}, 30 min), subsequently, the precipitates of Hemin-Au@MOF composites were collected and stored at 4 °C for future usage.

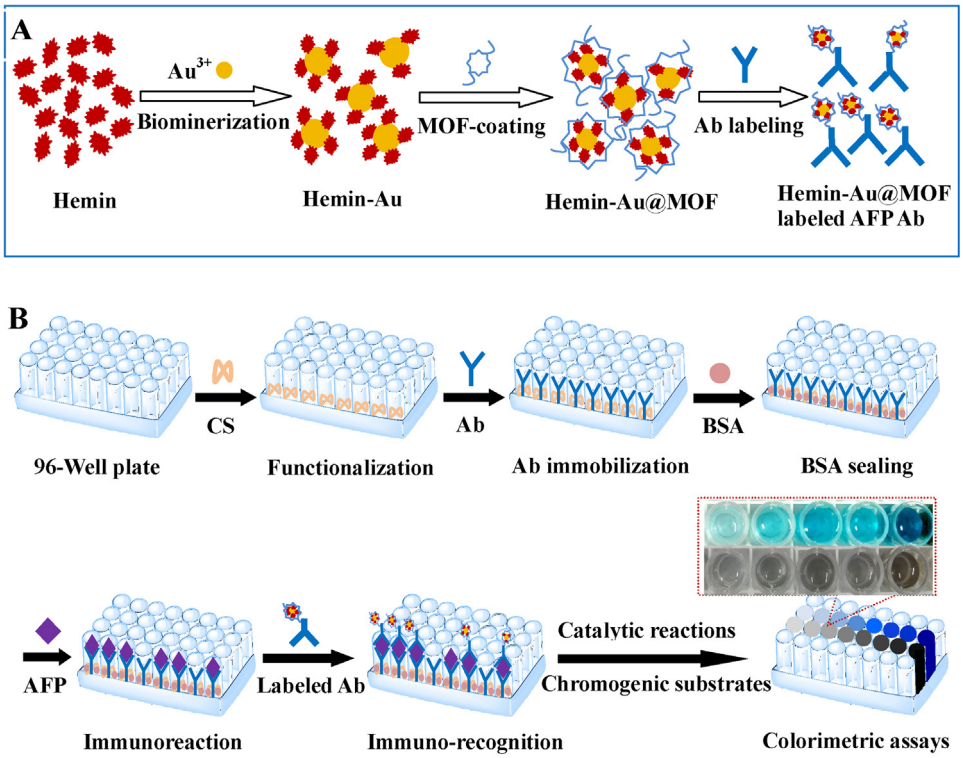

Scheme 1. Scheminatic illustration of (A) the fabrication procedure of Hemin-Au@MOF for labeling AFP antibody (Ab), including the hemin-mediated Au biomineriation yielding Hemin-Au, the coating of Tb-MOFs forming Hemin-Au@MOF, and the labeling of AFP Ab; (B) the colorimetric detection procedure with 96-well plate for probing AFP, including the CS functionalization, Ab immobilization, BSA sealing, antibody-antigen immunoreaction, immune-recognition with Hemin-Au@MOF labeled Ab, and the Hemin-Au-catalyzed reactions separately using chromogenic reaction substrates of TMB-H_2O_2 and Ag deposition, showing the high-throughput analysis for AFP of different levels in blood.

2.3. Colorimetric studies on Hemin-Au@MOF

Typically, an aliquot of the prepared Hemin-Au@MOF composites was introduced into the TMB-H_2O_2 substrates to catalyze the chromogenic reactions for 20 min, of which the blue reaction products were monitored by recording the UV–vis absorbance values at 652 nm using 96-well plates. The main conditions for the synthesis of Hemin-Au@MOF composites were first optimized using different molar ratios of hemin to Au dosages (81/5000, 81/2500, 81/1250, 81/1000, 81/625, 81/500, 243/1250, and 243/1000) and Hemin-Au to Tb-MOF (13/250, 13/500, 13/1000, 13/1500, 13/2000, 13/2500, 13/3000, 13/4000, and 13/5000). Moreover, the Hemin-Au@MOF-catalysis reaction conditions were performed using TMB-H_2O_2 substrates at different hemin dosages (0.025, 0.05, 0.15, 0.25, 0.35, 0.45, 0.50, 0.625, 0.75, 0.85, and 1.0 mg mL^{-1}), ionic strength (0.020, 0.040, 0.050, 0.060, 0.080, 0.10, 0.12, 0.15, 0.18, and 0.20 M), reaction temperature (0, 10, 20, 30, 37, 45, 60, and 75 °C), and pH values (2, 4, 6, 8, 10, 12, and 14). Meanwhile, the colorimetric investigations were carried out accordingly for exploring the enzymatic catalysis activities of Hemin-Au@MOF composites separately comparing to native hemin and Hemin-Au, each containing the same concentration of hemin, which was determined according to the results of the UV–vis absorbance measurements by referring to the plotted standard hemin concentration-absorbance curves. Further, the investigations of catalysis stability of Hemin-Au@MOF composites were carried out including the catalytic reaction and storage time. In addition, the steady state kinetic studies by colorimetric measurements were comparably conducted for Hemin-Au@MOF composite and native hemin, each containing 2.0 μg mL^{-1} hemin, where 4.41 mM H_2O_2 or 0.42 mM TMB was used alternatively at a fixed concentration of one substrate versus varying concentrations of the second substrate. Subsequently, the Lineweaver-Burk plots were performed for calculating the Michaelis-Menten constants, where the double-reciprocal plots for kinetic catalysis of Hemin-Au@MOF were carried separately by using various TMB concentrations at three fixed H_2O_2 concentrations (0.50, 3.5, and 7.5 mM) and the diverse H_2O_2 concentrations at three fixed TMB concentrations (0.28, 0.55, and 0.75 mM).

2.4. The 96-well plates-based immunoassays for AFP in blood

The synthesis of Hemin-Au@MOF-labeled anti-AFP antibodies was firstly performed by the activation of Hemin-Au@MOF with free carboxyl groups for cross-linking anti-AFP antibodies. Briefly, the EDC/NHS mixture (0.10 M, pH 5.0) was added to the Hemin-Au@MOF solution (0.016 mg mL^{-1}) to be incubated at room temperature for 30 min. After being washed twice, the activated Hemin-Au@MOF composites were mixed with anti-AFP antibody (3.0 μg mL^{-1}) to be incubated at 4 °C overnight, followed by being washed twice. Furthermore, the optimization of main immunoassay conditions for probing AFP was performed using different Hemin-Au@MOF concentrations (0.25, 0.50, 0.75, 1.0, 1.25, 1.5, 1.75, and 2.0 mg mL^{-1}), hybridization time (10, 20, 30, 40, 50, 60, 70, and 80 min), $AgNO_3$ dosages (0.25, 0.50, 1.0, 1.25, 1.5, 1.75, 2.0, 2.25, 2.5, 2.75, and 3.0 mM), and silver deposition time (2, 4, 6, 8, 10, 12, 14, and 16 min). Subsequently, the sandwiched immunoassays with the 96-well plates were conducted for different concentrations of AFP spiked in blood. Basically, the substrates of 96-well plates were first modified with CS to be derivatized with amine groups for the further covalent immobilization of anti-AFP antibody. An aliquot of anti-AFP antibody (0.30 g mL^{-1}) containing 2.5% glycerol and 0.0040% triton X-100 was separately dropped on the testing wells to be incubated for 8 h at room temperature. After being rinsed twice with PBS, 0.10% BSA was used to be incubated

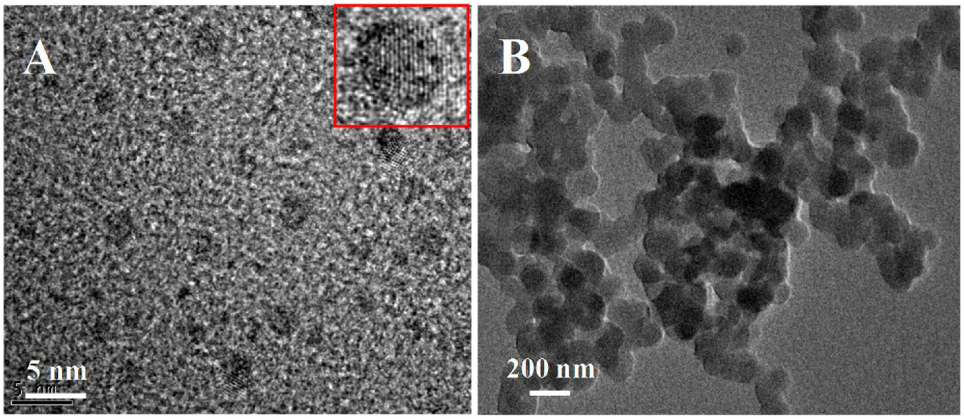

Fig. 1. TEM images for (A) Hemin-Au (insert: a particle with magnitude-amplified view), (B) Hemin-Au@MOF, each containing 2.0 μg mL^{-1} hemin.

for 1 h to block any active points that might conduct the nonspecific protein binding. Furthermore, an aliquot of human AFP of various concentrations in blood was separately added to the testing wells to be incubated for 1 h at 37 °C. After being rinsed with 0.010 M PBS twice, an aliquot of Hemin-Au@MOF-labeled anti-AFP antibody (3.0 μg mL^{-1}) was separately introduced to be further incubated for 1 h at 37 °C, and then washed twice. Subsequently, the colorimetric AFP detections were conducted for the silver deposition-based immunoassays with 96-well plates separately using an aliquot of TMB-H_2O_2 substrates and silver deposition substrates.

3. Result and discussion

3.1. Synthesis and characterization of Hemin-Au@MOF composites

It has been widely recognized that hemin as the active center of hemin-containing proteins can possess the peroxidase-like catalysis, but may encounter with some inherent limitations aforementioned, leading to considerably low catalysis activity and environmental robustness [16]. In the present work, hemin was employed as the stabilizer and reducing scaffold for the in-site biomineralization of small gold to form the Hemin-Au core, and further shelled with the protective skeletons of Tb-MOF matrix to form Hemin-Au@MOF composites, with the main fabrication route schematically illustrated in Scheme 1A. Herein, Au ions would first react with the functional groups of hemin scaffold like pyrroles, and then in site biomineralized to yield the Hemin-Au cores. Further, the Tb metal precursor was introduced to chelate with the carboxyl group of hemin of Hemin-Au to form a complex, followed by the reaction with terephthalic acid disodium, yielding the Hemin-Au@MOF composites with free carboxyl groups. On the one hand, the biomineralized gold would act as "nanowires" to promote the electron shuttling of the catalysis-active site of hemin in Hemin-Au@MOF composites. On the other hand, they would substantially cause the conformational change of Hemin-Au@MOF to create the reactivity pathways for pre-organizing more substrates to the catalysis active sites [21]. Meanwhile, the MOF shelled on the Hemin-Au cores would serve as the protective skeletons to guarantee the improved catalysis properties and high environmental robustness of Hemin-Au. Furthermore, the so prepared Hemin-Au@MOF composites would be expected to present the double catalysis activities of peroxidase-like and gold catalysis to serve as the catalytic labels for modifying anti-AFP antibody (Ab). A high-throughput sandwiched colorimetric immunoassay method with 96-well plates was thereby developed for probing AFP in blood separately through the two signal amplification ways of ELISA and GCSS. As shown in Scheme 1B, AFP in blood would be first captured by anti-AFP Ab, which was immobilized on the chitosan (CS) derivatized 96-well plates, followed by the further recognition of Hemin-Au@MOF-labeled anti-AFP Ab. Subsequently, either of the hemin-catalyzed TMB-H_2O_2 chromogenic reaction or gold-catalyzed silver deposition route was conducted for the 96-well plates-based sandwiched immunoassays for AFP in blood.

The topological structure of the developed Hemin-Au@MOF composites was characterized by transmission electron microscope (TEM) imaging (Fig. 1). One can note from Fig. 1A that Hemin-Au cores were highly uniform and well dispersed in water, showing an average particle size of about 2.0–3.0 nm in diameter. The catalysis-active hemin could be anchored onto the biomineralized gold with clear crystalline lattices as apparently manifested in the magnitude-amplified view (Fig. 1A, insert). Furthermore, as can be seen from Fig. 1B, the obtained Hemin-Au@MOF composites could be formed to exhibit the well-defined particles with the size of about 200 nm in diameter, thus promising the GCSS-based colorimetric immunoassay for AFP as demonstrated afterwards.

Moreover, UV–vis spectra were recorded for the developed Hemin-Au@MOF composites by taking native hemin and Tb-MOF as the comparison (Fig. 2A). One can note that Hemin-Au@MOF composites (curve d) could include the absorption peaks of hemin (curve b, about 385 nm) and biomineralized gold compound (about 330 nm), so did the Hemin-Au cores (curve c), thus confirming the successful reconstitution of Hemin-Au@MOF. Of note, the Tb-MOF (curve a) could show no apparent surface plasmon resonance over the measured absorbance range.

3.2. Colorimetric investigations of Hemin-Au@MOF composites

Colorimetric studies were carried out for the catalysis performances of Hemin-Au@MOF composites by comparing to native hemin and Hemin-Au (Fig. 2B). The results of the catalytic TMB-H_2O_2 reactions indicate that Hemin-Au@MOF could display over four-fold stronger catalysis activity than native hemin, but approximate to that of Hemin-Au, as clearly witnessed in the photographs of the reaction product solutions (insert). At the meantime, Hemin-Au@MOF can present the gold catalysis for catalyzing the silver deposition, as also disclosed in the photographs of sliver staining products of sliver staining products showing the corresponding UV–vis absorption. Herein, the biomineralized gold of Hemin-Au@MOF would accelerate the electron transferring of Hemin-Au@MOF, together with enhanced affinity for the reactive substrates aforementioned. In addition, the encapsulated gold of Hemin-Au@MOF could catalyze the silver deposition reaction to facilitate the GCSS-based immunoassay, which would achieve more

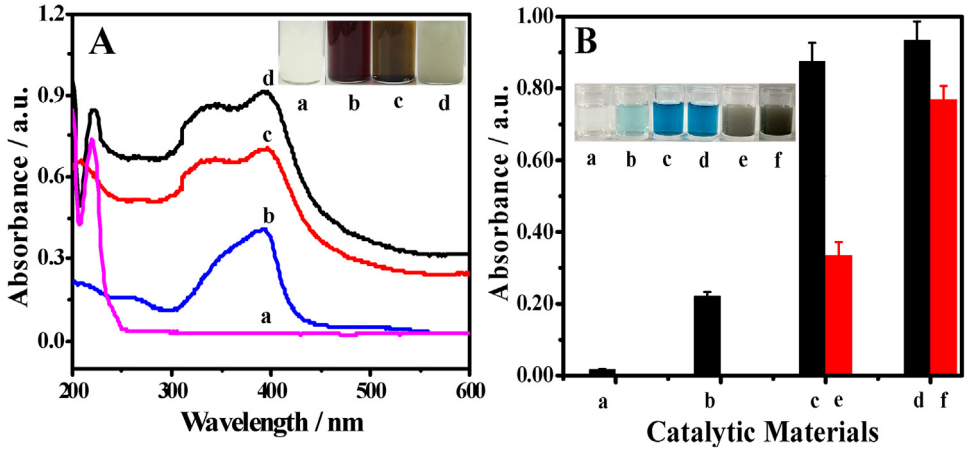

Fig. 2. (A) UV–vis spectra of (a) MOF (Tb), (b) Hemin, (c) Hemin-Au, and (d) Hemin-Au@MOF, with the photographs of corresponding catalytic materials (insert), (B) The activities in catalyzing TMB-H_2O_2 (1.6 mM H_2O_2, 0.62 mM TMB) reactions of (a) blank, (b) Hemin, (c) Hemin-Au, (d) Hemin-Au@MOF, and (e) Hemin-Au and (f) Hemin-Au@MOF-catalyzed silver deposition (10 mM Hemin-Au@MOF, 2.0 mM $AgNO_3$, 0.57 mM vitamin C), with the photographs of corresponding product solutions (insert) and each containing 2.0 μg mL^{-1} hemin. All results were the average values of five replicates.

than about 2.3 times higher responses than those of the ones using Hemin-Au label. Therefore, the developed Hemin-Au@MOF composites could possess the enhanced double catalysis activities of peroxidase-like and gold catalysis for the catalysis-based sandwiched immunoassays for AFP afterwards.

3.3. Optimization of the main conditions of the fabrication of Hemin-Au@MOF catalysts

The main experimental conditions for the synthesis of Hemin-Au@MOF composites were optimized with the results shown in Fig. 3. Apparently, the catalysis performances of Hemin-Au@MOF composites could depend on the molar ratios of hemin to Au used in the synthesis reactions, showing the optimal catalysis at the one of 81/625 (Fig. 3A). Meanwhile, the dosages of Hemin-Au to Tb-MOF for the synthesis of Hemin-Au@MOF were explored (Fig. 3B). One can find that the Hemin-Au to Tb-MOF ratio of about 13/2000 should be the optimum one to be selected for forming Hemin-Au@MOF composites.

Colorimetric studies were conducted on the peroxidase-like catalysis activities of Hemin-Au@MOF composites in comparison with native hemin and Hemin-Au under different reaction conditions, mainly including the dosages of hemin, ion strengths, pH values, and temperature (Fig. 4). It was found that the Hemin-Au@MOF could display the same dosage-dependent catalysis behavior as Hemin-Au and native hemin, except for much higher catalysis ability (Fig. 4A). Also, both of them could allow for the catalytic TMB-H_2O_2 reactions occurring at the optimal ion strength of 0.10 M NaCl (Fig. 4B), temperature of about 37 °C (Fig. 4C), and pH 6.0 (Fig. 4D), which are well consistent with these real conditions of the biological systems. More importantly, the Hemin-Au@MOF may maintain high catalytic activities over a wide range of temperature and pH values, showing the wonderful applicability for various catalysis applications. Furthermore, Fig. 5A reveals that the Hemin-Au@MOF could display much faster catalysis reaction than native hemin but similar to Hemin-Au. Much improved storage stabilities of Hemin-Au@MOF could also be expected, showing no significant change of catalysis performances when stored in water up to one year (Fig. 5**B**). These results indicate that the prepared Hemin-Au@MOF could exhibit much enhanced double catalysis activities and high environmental stability in the five replicated tests.

Table 1
Comparison of dynamic catalysis parameters among hemin, Hemin-Au@MOF, and HRP documented in catalyzing the TMB-H_2O_2 reactions.

Catalysis materials	Substrates	K_m (mM)
Hemin	TMB	5.23
Hemin-Au@MOF	TMB	2.67
HRP	TMB	0.434
Hemin	H_2O_2	4.06
Hemin-Au@MOF	H_2O_2	2.58
HRP	H_2O_2	3.70

3.4. Studies on steady-state catalysis kinetics of Hemin-Au@MOF

Colorimetric dynamic studies were performed for the developed Hemin-Au@MOF using the TMB-H_2O_2 reaction system, taking native hemin as the comparison (Fig. 6). Fig. 6A describes that the Hemin-Au@MOF could facilitate much better catalytic performances than native hemin in terms of catalytic reaction rates and response range of H_2O_2 concentrations. In particular, the developed composites could tolerate toxic H_2O_2 up to 35 mM without any significant change of catalysis activities. Also, the Hemin-Au@MOF could display much better catalysis responses in the TMB-H_2O_2 reactions with various TMB concentrations (Fig. 6B). Furthermore, kinetic parameters of steady-state catalysis were obtained for the Hemin-Au@MOF in comparison with native hemin (Fig. 6C and D). Herein, the apparent Michaelis constants (K_m) were calculated by using Lineweaver-Burk plots of the double reciprocal of the Michaelis-Menten equation, of which the double reciprocal curves involved were comparably shown for varying substrates of H_2O_2 and TMB. The so yielded kinetic parameters are comparably summarized in Table 1. Accordingly, the apparent K_m for TMB substrate of Hemin-Au@MOF (2.67 mM) was much lower than that of native hemin (5.23 mM), indicating that Hemin-Au@MOF may possess a higher affinity for TMB. Moreover, the K_m of Hemin-Au@MOF for H_2O_2 substrate (2.58 mM) is also much lower than that of native hemin (4.06 mM). Additionally, comparing to other kind of hemin composites like hemin-graphene hybrids reported elsewhere [16], the as-prepared Hemin-Au@MOF could display a lower K_m for TMB substrate and appropriate K_m for H_2O_2 substrate. Furthermore, the possible catalysis mechanism of Hemin-Au@MOF was investigated for catalyzing the TMB-H_2O_2 reaction. The double reciprocal plots of initial velocities against three fixed concentrations of one substrate were obtained over a range of concentrations of another substrate separately for TMB and H_2O_2 (Fig. 6E and F).

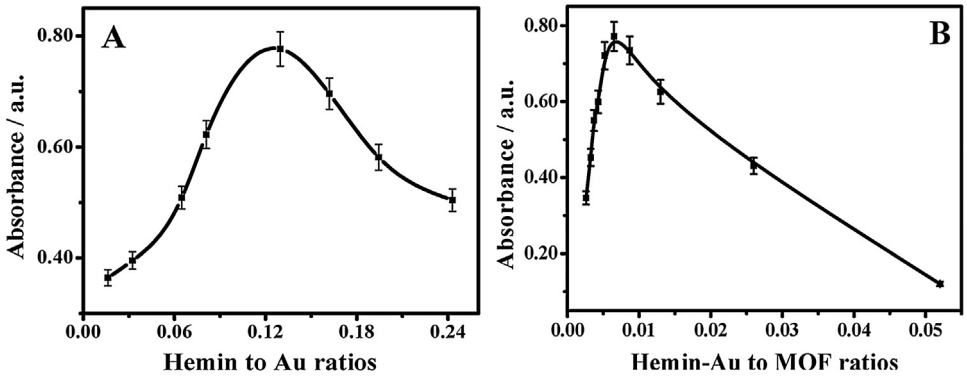

Fig. 3. Colorimetric investigation on the main conditions for the synthesis of Hemin-Au@MOF with the catalysis activities depending on (A) Hemin to Au molar ratios and (B) Hemin-Au to MOF molar ratios, where the synthesis of Hemin-Au@MOF were performed using different molar ratios of hemin (0.13 mM), $HAuCl_4$ (1.0 mM), and Tb-MOF (10 mM).

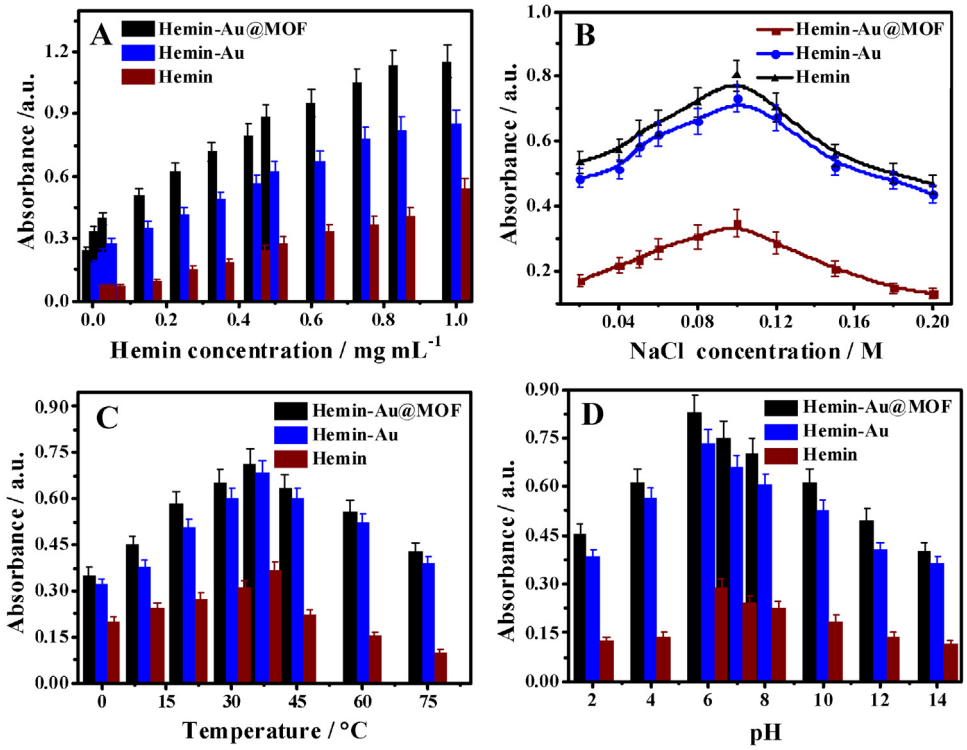

Fig. 4. The optimization of catalysis reaction conditions of the Hemin-Au@MOF-based colorimetric analysis including (A) different hemin concentrations; (B) different NaCl concentrations; (C) different temperature, and (D) pH values, taking hemin and Hemin-Au as the comparison. All results were the average values of five replicates.

As expected, the characteristic catalysis of Hemin-Au@MOF could feature a ping-pong mechanism, as confirmed elsewhere for HRP [39]. Therefore, these data demonstrate that the developed Hemin-Au@MOF could present stronger peroxidase-like catalysis activity than native hemin, thus promising for a broad range of catalysis applications.

3.5. Optimization of the main conditions for the Hemin-Au@MOF-based AFP immunoassays

The colorimetric investigations were conducted for optimizing the experimental conditions for the AFP immunoassays with the signal amplification by the exemplified GCSS route (Fig. 7). It was discovered that the absorbance values could depend on the dosages of Hemin-Au@MOF, showing the most suitable concentration of 1.0 mg mL^{-1} (Fig. 7A). Also, the sandwiched immune-reaction time was explored (Fig. 7B). Obviously, the absorbance of deposited silver could tend to be steady after 50 min, which is thus chosen for the immune-reactions. Furthermore, investigations were carried out on the amounts of $AgNO_3$, with the data manifested in Fig. 7C. One can find that the silver signals could increase with the increasing concentrations of $AgNO_3$ till reaching the constant responses up to 2.0 mM. In addition, Fig. 7D displays the deposition time-dependent silver signals, showing that 10 min is enough for the silver deposition. Accordingly, the existence of Au in the Hemin-Au@MOF could not only help to enhance the catalysis activity of Hemin-Au@MOF aforementioned, but also act as the catalyst for catalyzing the silver deposition reaction so as to facilitate the GCSS-based colorimetric immunoassays for AFP.

3.6. Preliminary catalysis applications in immunoassay

The feasibility of the developed colorimetric immunoassays with Hemin-Au@MOF were investigated for probing AFP in blood

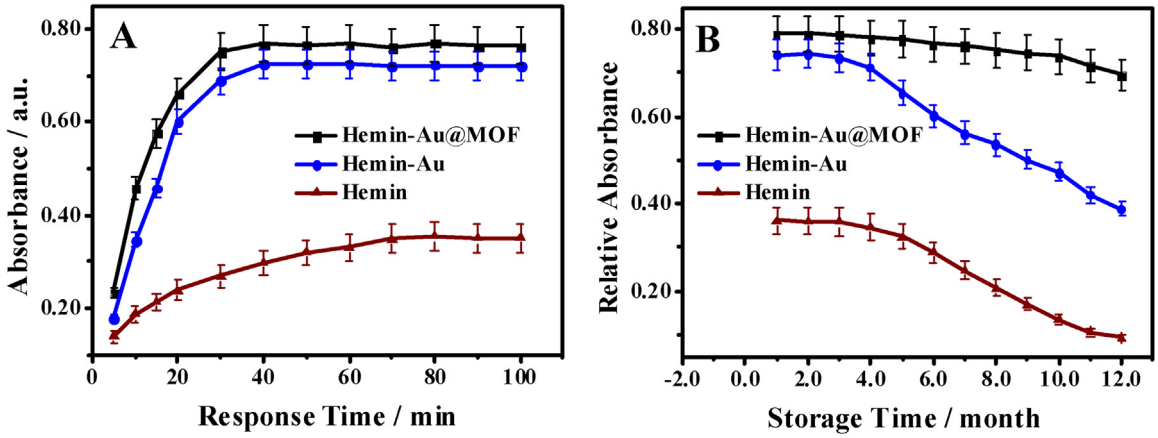

Fig. 5. (A) The time-depending colorimetric responses of TMB-H_2O_2 reactions catalyzed by Hemin-Au@MOF composite in comparison to hemin. (B) The environmental stability of Hemin-Au@MOF stored in water over different time intervals, where the catalytic TMB-H_2O_2 reactions were performed for monitoring the catalytic activities of Hemin-Au@MOF using 1.6 mM H_2O_2 and 0.62 mM TMB, taking hemin and Hemin-Au as the comparison. All results were the average values of five replicates.

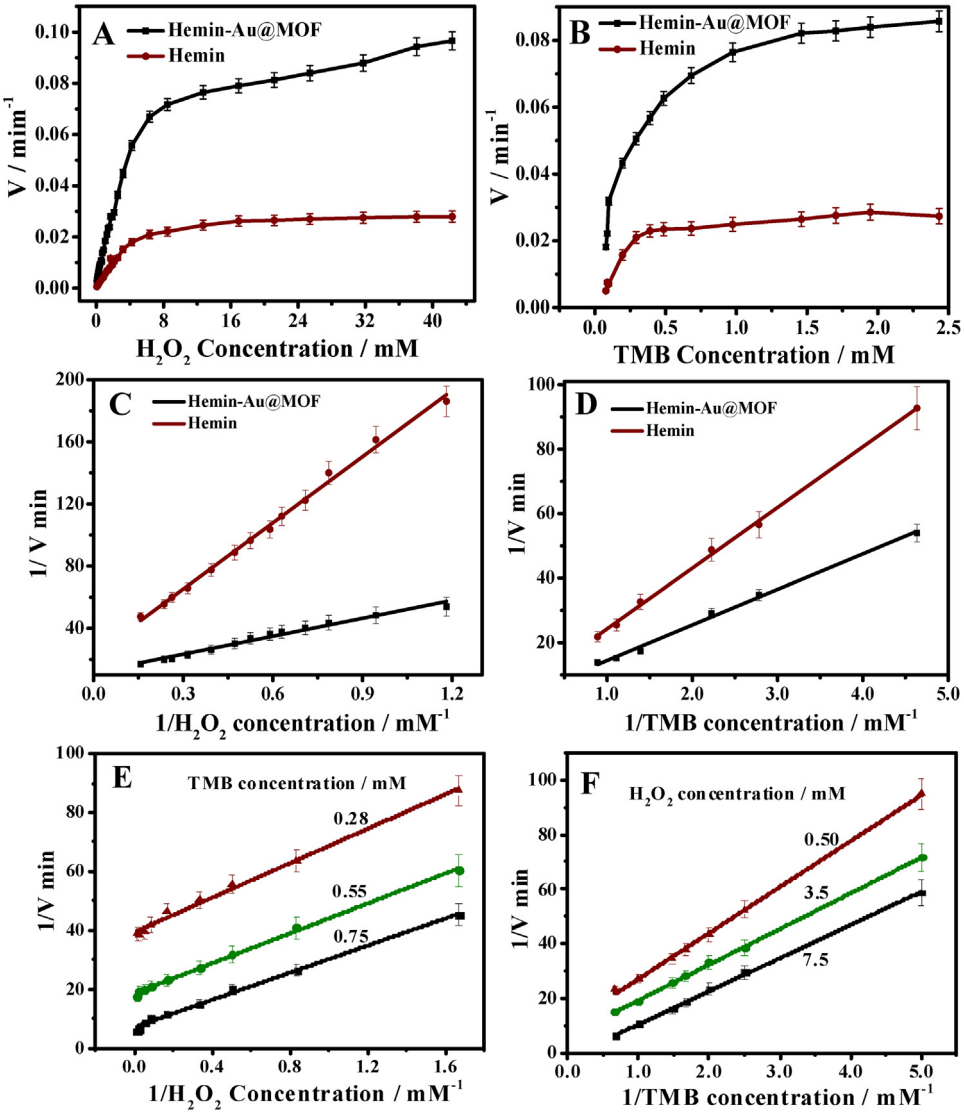

Fig. 6. Catalysis kinetics for Hemin-Au@MOF with (A) H_2O_2 and (B) TMB concentrations-dependent colorimetric responses using 0.42 mM TMB and 4.41 mM H_2O_2, respectively, taking hemin as the comparison. Double-reciprocal plots for the comparison of catalysis activities between Hemin-Au composite (red) and hemin (black) using (C) various H_2O_2 concentrations at fixed 0.42 mM TMB and (D) various TMB concentrations at fixed 4.41 mM H_2O_2. The double-reciprocal plots for catalysis kinetics of Hemin-Au composite using (E) various H_2O_2 concentrations at three fixed TMB concentrations, and (F) various TMB concentrations at three fixed H_2O_2 concentrations. The y-axis values were calculated from the colorimetric absorbance values recorded. All results were the average values of five replicates. (For interpretation of the references to colour in this figure legend, the reader is referred to the web version of this article.)

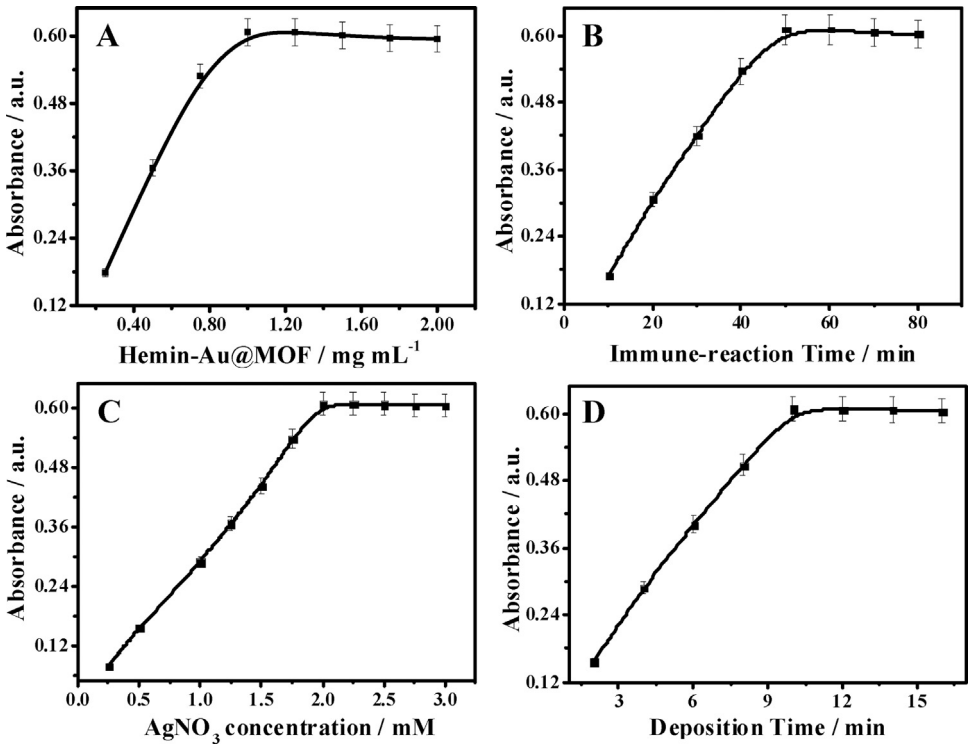

Fig. 7. Optimization of the main immunoassay conditions of (A) Hemin-Au@MOF concentrations, (B) immune-reaction time, (C) $AgNO_3$ dosages, and (D) deposition time using 25 ng mL^{-1} of AFP.

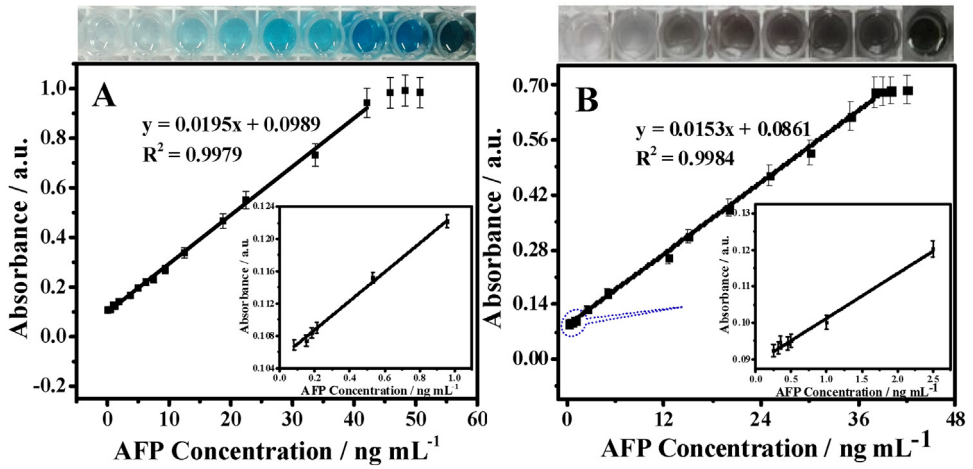

Fig. 8. The calibration curves of the Hemin-Au@MOF catalysis-based colorimetric method for the detection of AFP with different concentrations using (A) TMB-H_2O_2 substrate (1.6 mM H_2O_2, 0.62 mM TMB) and (B) silver deposition substrate (2.0 mM $AgNO_3$, 0.57 mM vitamin C), with the error bars of five replicates showing the standard deviations and the photographs of the product solutions of corresponding reactions (insert), where the curves were obtained separately by plotting the colorimetric responses versus different AFP concentrations from 0.08 to 42.8 ng mL^{-1} and 0.25–38 ng mL^{-1}, respectively.

separately by the ELISA and GCSS signal amplification ways, of which five replicated tests for targeting AFP were conducted (Fig. 8). Fig. 8A manifests the calibration curve of the Hemin-Au@MOF-based ELISA immunoassays by the catalytic chromogenic reactions for different concentrations of AFP spiked in blood. Accordingly, AFP can be detected in the concentrations linearly ranging from 0.080 to 43 ng mL^{-1}, with a high correlation coefficient (R^2 = 0.9979). A detection limit of about 0.020 ng mL^{-1} was obtained as estimated by the 3σ rule, which performance is comparable to that of the colorimetric ELISA method reported elsewhere [4]. Moreover, the GCSS-based sandwiched immunoassay was conducted by the catalytic silver staining route for probing AFP in blood. Fig. 8B shows the dose-response curve describing the absorbance values of deposited silver versus different AFP concentrations. A detection range is obtained for AFP concentrations ranging from 0.25 to 38 ng mL^{-1}, with a limit of detection about 0.10 ng mL^{-1}, as clearly disclosed with the typical photographs (Fig. 8B, insert). Moreover, as compared to some other AFP analysis methods reported previously [4,40,41], the developed Hemin-Au@MOF-based colorimetric immunoassay method can present the better or compatible detection performances in terms of linear detection range and detection limit (Table 2). Also, higher detection reproducibility of the developed colorimetric method was demonstrated showing no significant change in the five repeated tests (data not shown).

Table 2
Comparison of detection performances among the different analysis methods for AFP.

Analysis methods	Linear ranges ($ng\,mL^{-1}$)	Detection limit ($ng\,mL^{-1}$)
Colorimetric Analysis [4]	0.20–20	0.10
Localized surface plasmon resonance [40]	20–200	24
Photoelectrochemical [41]	0.10–500	0.01
This Work	0.08–43	0.02
	0.25–38	0.10

Therefore, the so developed Hemin-Au@MOF-based colorimetric strategies could promise for the practical applications for the highly throughput and sensitive analysis for AFP in blood.

4. Conclusion

To summarize, a simple and efficient enzymatic fabrication protocol has been successfully developed by remolding the catalytic hemin with biomineralized gold to form Hemin-Au core to be further encapsulated into the Tb-MOF, yielding the Hemin-Au@MOF composites. As evidenced in the colorimetric assays, the obtained Hemin-Au@MOF could possess robust environmental stability and especially double catalysis activities of enhanced peroxidase-like and gold catalysis. Steady-state kinetics studies indicate that comparing to native hemin and even natural peroxidases like HRP, the Hemin-Au@MOF could present much higher intrinsic catalysis (over four-fold stronger than that of native hemin) and substrate affinity (lower Michaelis constants). Herein, the biomineralized gold would promote the electron transferring of Hemin-Au@MOF. The conformational changes of Hemin-Au@MOF would also be triggered so as to create the reactivity pathways for pre-organizing more substrates toward the active sites. Meanwhile, the MOF shelled on the Hemin-Au cores would serve as the protective skeletons to guarantee the improved catalysis properties and environmental robustness of Hemin-Au@MOF. Furthermore, the developed catalytic composites were employed to label anti-AFP antibodies for the sandwiched immunoassays with 96-well plates for explore AFP in blood. The analysis results indicate that the Hemin-Au@MOF-based immunoassays could allow for the highly sensitive AFP analysis by two signal amplification ways of hemin-catalyzed chromogenic reaction or gold-catalyzed silver staining. Besides, by combining the gold biomineralization and MOF encapsulation routes, the proposed enzymatic fabrication protocol may open a new door toward the efficient preparation or enhancement of a variety of robust enzymes or enzymatic mimics with the improved environmental stability and multiple catalysis activities, thus promising the wide applications in the catalysis-based biomedical analysis, food safety, and environmental monitoring fields.

Acknowledgements

This work is supported by the National Natural Science Foundation of China (No. 21675099, and 21375075), Science and Technology Development Project of Weihai (2015DXGJZD002), and the Taishan Scholar Foundation of Shandong Province, P. R. China.

References

[1] P.R. Srinivas, B.S. Kramer, S. Srivastava, Trends in biomarker research for cancer detection, Lancet Oncol. 2 (2001) 698–704.
[2] X.Y. Yang, Y.S. Guo, S. Bi, S.S. Zhang, Ultrasensitive enhanced chemiluminescence enzyme immunoassay for the determination of α-fetoprotein amplified by double-codified gold nanoparticles labels, Biosens. Bioelectron. 24 (2009) 2707–2711.
[3] W. Li, X. Jiang, J. Xue, Z. Zhou, J. Zhou, Antibody modified gold nano-mushroom arrays for rapid detection of alpha-fetoprotein, Biosens. Bioelectron. 68 (2015) 468–474.
[4] W.H. Zhou, C.L. Zhu, C.H. Lu, X.C. Guo, F.R. Chen, H.H. Yang, X.R. Wang, Amplified detection of protein cancer biomarkers using DNAzyme functionalized nanoprobes, Chem. Commun. 0 (2009) 6845–6847.
[5] Y. Nagasaki, H. Kobayashi, Y. Katsuyama, T. Jomura, T. Sakura, Enhanced immunoresponse of antibody/mixed-PEG co-immobilized surface construction of high-performance immunomagnetic ELISA system, J. Colloid Interf. Sci. 309 (2007) 524–530.
[6] M. Hamzawy, L. Elsaid, A. Shams, L. Rashid, S. Mahfouz, N. Sharawy, Study of the effects of cyclooxygenase-2 inhibitor on the promotion of hepatic tumorigenesis in rats fed a high fat diet, J. Clin. Exp. Hepatol. 5 (2015) 14–21.
[7] R. Li, S.Y. Li, M.M. Dong, L.Y. Zhang, Y.C. Qiao, Y. Jiang, W. Qi, H. Wang, A highly specific and sensitive electroanalytical strategy for microRNAs based on amplified silver deposition by the synergic TiO_2 photocatalysis and guanine photoreduction using charge-neutral probes, Chem. Commun. 51 (2015) 16131–16134.
[8] Y.M. Si, Z.Z. Sun, N. Zhang, W. Qi, S. Li, L.J. Chen, H. Wang, Ultrasensitive electroanalysis of low-level free microRNAs in blood by maximum signal amplification of catalytic silver deposition using alkaline phosphatase-incorporated gold nanoclusters, Anal. Chem. 86 (2014) 10406–10414.
[9] R.M. Lequin, Enzyme immunoassay (EIA)/enzyme-linked immunosorbent assay (ELISA), Clin. Chem. 51 (2005) 2415–2418.
[10] C. Li, Y.C. Yang, D. Wu, T.Q. Li, Y.M. Yin, G.X. Li, Improvement of enzyme-linked immunosorbent assay for multicolor detection of biomarkers, Chem. Sci. 7 (2016) 3011–3016.
[11] D.J. Lin, J. Wu, M. Wang, F. Yan, H.X. Ju, Triple signal amplification of graphene film, polybead carried gold nanoparticles as tracing tag and silver deposition for ultrasensitive electrochemical immunosensing, Anal. Chem. 84 (2012) 3662–3668.
[12] J. Li, S. Song, X. Liu, L. Wang, D. Pan, Q. Huang, Y. Zhao, C. Fan, Enzyme-based multi-component optical nanoprobes for sequence-specific detection of DNA hybridization, Adv. Mater. 20 (2008) 497–500.
[13] D.P. Tang, J.J. Ren, In situ amplified electrochemical immunoassay for carcinoembryonic antigen using horseradish peroxidase-encapsulated nanogold hollow microspheres as labels, Anal. Chem. 80 (2008) 8064–8070.
[14] J. Wu, Z.F. Fu, F. Yan, H.X. Ju, Biomedical and clinical applications of immunoassays and immunosensors for tumor markers, Trends Anal. Chem. 26 (2007) 679–688.
[15] H. Wei, E.K. Wang, Nanomaterials with enzyme-like characteristics (nanozymes): next-generation artificial enzymes, Chem. Soc. Rev. 42 (2013) 6060–6093.
[16] Y.J. Guo, L. Deng, J. Li, S.J. Guo, E.K. Wang, S.J. Dong, Hemin-graphene hybrid nanosheets with intrinsic peroxidase-like activity for label-free colorimetric detection of single-nucleotide polymorphism, ACS Nano 5 (2011) 1282–1290.
[17] F. Valentini, L. Cristofanilli, M. Carbone, G. Palleschi, Glassy carbon electrodes modified with hemin-carbon nanomaterial films for amperometric H_2O_2 and NO_2-detection, Electrochim. Acta 4 (2012) 187–201.
[18] A.M. Toader, E. Volanschi, Electrochemical and spectral study of the hemin-surfactant interaction in solution, Rev. Roum. Chim. 52 (2007) 159–167.
[19] M.S. Mizrachi, G.M. Pavan, E. Levin, A. Danani, N.G. Lemcoff, Catalytic chameleon dendrimers, J. Am. Chem. Soc. 133 (2011) 14359–14367.
[20] M.M. Dong, L.Y. Zhang, R. Li, S.Y. Li, Y. Jiang, Y.C. Qiao, Z.Q. Duan, R. Li, Q.F. Wang, H. Wang, Crosslinking catalysis-active center of hemin on the protein scaffold toward peroxidase mimic with powerful catalysis, RSC Adv. 6 (2016) 47595–47599.
[21] L.Y. Zhang, S. Li, M.M. Dong, Y. Jiang, R. Li, S. Zhang, X.X. Lv, L.J. Chen, H. Wang, Reconstituting redox active centers of heme-containing proteins with biomineralized gold toward peroxidase mimics with strong intrinsic catalysis and electrocatalysis for H_2O_2 detection, Biosens. Bioelectron. 87 (2017) 1036–1043.
[22] T. Xue, S. Jiang, Y.Q. Qu, Q. Su, R. Cheng, S. Dubin, C.Y. Chin, R. Kaner, Y. Huang, X.F. Duan, Graphene-supported hemin as a highly active biomimetic oxidation catalyst, Angew. Chem. Int. Ed. 124 (2012) 3888–3891.
[23] J. Wang, D.K. Xu, R. Polsky, Magnetically-induced solid-state electrochemical detection of DNA hybridization, J. Am. Chem. Soc. 124 (2002) 4208–4209.
[24] S.J. Park, T.A. Taton, C.A. Mirkin, Array-based electrical detection of DNA with nanoparticle probes, Science 295 (2002) 1503–1506.
[25] X. Zhou, S.J. Xia, Z.Q. Lu, Y. Tian, Y.S. Yan, J. Zhu, Biomineralization-assisted ultrasensitive detection of DNA, J. Am. Chem. Soc. 132 (2010) 6932–6934.
[26] S.I. Stoeva, J.S. Lee, J.E. Smith, S.T. Rosen, C.A. Mirkin, Multiplexed detection of protein cancer markers with biobarcoded nanoparticle probes, J. Am. Chem. Soc. 128 (2006) 8378–8379.
[27] S. Lee, C.Y. Fan, T.P. Wu, S.L. Anderson, CO oxidation on Au_n/TiO_2 catalysts produced by size-selected cluster deposition, J. Am. Chem. Soc. 126 (2004) 5682–5683.
[28] X.X. Wang, Q. Wu, Z. Shan, Q.M. Huang, BSA-stabilized Au clusters as peroxidase mimetics for use in xanthine detection, Biosens. Bioelectron. 26 (2011) 3614–3619.
[29] A. Asati, S. Santra, C. Kaittanis, S. Nath, J.M. Perez, Oxidase-like activity of polymer-coated cerium oxide nanoparticles, Angew. Chem. Int. Ed. 121 (2009) 2344–2348.

[30] S.S. Wang, Z.P. Chen, J. Choo, L.X. Chen, Naked-eye sensitive ELISA-like assay based on gold-enhanced peroxidase-like immunogold activity, Anal. Bioanal. Chem. 408 (2016) 1015–1022.
[31] S.R. Ahmed, K. Takemeura, T.C. Li, N. Kitamoto, T. Tanaka, T. Suzuki, E.Y. Park, Size-controlled preparation of peroxidase-like graphene-gold nanoparticle hybrids for the visible detection of norovirus-like particles, Biosens. Bioelectron. 87 (2017) 558–565.
[32] B. Basnar, Y. Weizmann, Z. Cheglakov, I. Willner, Synthesis of nanowires using dip-pen nanolithography and biocatalytic inks, Adv. Mater. 18 (2010) 713–718.
[33] M.T. Zhao, K. Deng, L.C. He, Y. Liu, G.D. Li, H.J. Zhao, Z.Y. Tang, Core-shell palladium nanoparticle@metal-organic frameworks as multifunctional catalysts for cascade reactions, J. Am. Chem. Soc. 136 (2014) 1738–1741.
[34] L. Hamon, P.L. Llewellyn, T. Devic, A. Ghoufi, G. Clet, V. Guillerm, G.D. Pirngruber, G. Maurin, C. Serre, G. Driver, W.V. Beek, E. Jolimaître, A. Vimont, M. Daturi, G. Férey, Co-adsorption and separation of CO_2-CH_4 mixtures in the highly flexible MIL-53 (Cr) MOF, J. Am. Chem. Soc. 131 (2009) 17490–17499.
[35] X. Kuang, Y. Ma, H. Su, J. Zhang, Y.B. Dong, B. Tang, High-performance liquid chromatographic enantioseparation of racemic drugs based on homochiral metal-organic framework, Anal. Chem. 86 (2014) 1277–1281.
[36] L. Cui, J. Wu, J. Li, H.X. Ju, Electrochemical sensor for lead cation sensitized with a DNA functionalized porphyrinic metal-organic framework, Anal. Chem. 87 (2015) 10635–10641.
[37] K. Liang, R. Ricco, C.M. Doherty, M.J. Styles, S. Bell, N. Kirby, S. Mudie, D. Haylock, A.J. Hill, C.J. Doonan, P. Falcaro, Biomimetic mineralization of metal-organic frameworks as protective coatings for biomacromolecules, Nat. Commun. 6 (2015) 7240–7247.
[38] T.Z. Liu, R. Hu, X. Zhang, K.L. Zhang, Y. Liu, X.B. Zhang, R.Y. Bai, D.L. Li, Y.H. Yang, Metal-organic framework nanomaterials as novel signal probes for electron transfer mediated ultrasensitive electrochemical immunoassay, Anal. Chem. 88 (2016) 12516–12523.
[39] L.Z. Gao, J. Zhuang, L. Nie, J.B. Zhang, Y. Zhang, N. Gu, T.H. Wang, J. Feng, D.L. Yang, S. Perrett, X.Y. Yan, Intrinsic peroxidase-like activity of ferromagnetic nanoparticles, Nature Nanotech. 2 (2007) 577–583.
[40] W.B. Li, X.Q. Jiang, J.C. Xue, Z.K. Zhou, J.H. Zhou, Antibody modified gold nano-mushroom arrays for rapid detection of alpha-fetoprotein, Biosens. Bioelectron. 68 (2015) 468–474.
[41] R. Xu, Y.D. Jiang, L. Xia, T.X. Zhang, L. Xu, S. Zhang, D.L. Liu, H.W. Song, A sensitive photoelectrochemical biosensor for AFP detection based on ZnO inverse opal electrodes with signal amplification of CdS-QDs, Biosens. Bioelectron. 74 (2015) 411–417.

Biographies

Liyan Zhang received her master's degree in Analytical Chemistry at the College of Chemistry and Chemical Engineering in the Qufu Normal University in China, in 2017. Her research interests include Biosensors and Medical Detectors R&D.

Chuan Fan received his bachelor degree in Chemical Engineering and Technology from the Qufu Normal University, China, in 2015, and now is a postgraduate student in Analytical Chemistry at the College of Chemistry and Chemical Engineering in the same university. His research interests mainly include Biosensors and Medical Detectors R&D.

Min Liu received her bachelor degree in Chemical Engineering and Technology from the Qufu Normal University, China, in 2015, and now is a postgraduate student in Analytical Chemistry at the College of Chemistry and Chemical Engineering in the same university. His research interests mainly include Biosensors and Medical Detectors R&D.

Fengjuan Liu received her bachelor degree in Chemical Engineering and Technology from the Qufu Normal University, China, in 2015, and now is a postgraduate student in Analytical Chemistry at the College of Chemistry and Chemical Engineering in the same university. His research interests mainly include Biosensors and Medical Detectors R&D.

Shanshan Bian will receive her bachelor degree in Chemical Engineering and Technology from the Qufu Normal University, China, in 2018, and now is an undergraduate.

Shuyue Du will receive her bachelor degree in Chemical Engineering and Technology from the Qufu Normal University, China, in 2018, and now is an undergraduate.

Shuyun Zhu received her Ph.D from Changchun Institute of Applied Chemistry, Chinese Academy of Sciences, China, in 2012, and now is working at Qufu Normal University as an associate professor in Chemistry. Her research interests mainly include Biosensors and Medical Detectors R&D.

Hua Wang received his Ph.D from Hunan University, China, in 2004, and now is working at Qufu Normal University as a distinguished professor in Chemistry. His research interests mainly include Chemo/Biosensors, Advanced Functional Materials, and Organic Synthesis.